

This is the peer reviewed version of the following article: Wong, M. C., Chen, L., Bai, G., Huang, L. B., & Hao, J. (2017). Temporal and remote tuning of piezophotonic-effect-induced luminescence and color gamut via modulating magnetic field. *Advanced Materials*, 29(43), 1701945, which has been published in final form at <https://doi.org/10.1002/adma.201701945>. This article may be used for non-commercial purposes in accordance with Wiley Terms and Conditions for Use of Self-Archived Versions. This article may not be enhanced, enriched or otherwise transformed into a derivative work, without express permission from Wiley or by statutory rights under applicable legislation. Copyright notices must not be removed, obscured or modified. The article must be linked to Wiley's version of record on Wiley Online Library and any embedding, framing or otherwise making available the article or pages thereof by third parties from platforms, services and websites other than Wiley Online Library must be prohibited.

Temporal and remote tuning of piezophotonic effect-induced luminescence and color gamut via modulating magnetic field

*Man-Chung Wong, Li Chen, Gongxun Bai, Long-Biao Huang, Jianhua Hao\**

M.-C. Wong, L. Chen, Dr. G. X. Bai, Dr. L. B. Huang, Prof. J. H. Hao

Department of Applied Physics, The Hong Kong Polytechnic University, Kowloon, Hong Kong, P. R. China

The Hong Kong Polytechnic University Shenzhen Research Institute, Shenzhen 518057, P. R. China

Email: [jh.hao@polyu.edu.hk](mailto:jh.hao@polyu.edu.hk)

Keywords: piezophotonic effect, metal-ion doped phosphor, mechanoluminescence, magnetic sensor, RGB color

Luminescence materials have been extensively investigated because of their wide range of applications in display, solid state lighting, sensor, memory and bioimaging.<sup>[1-8]</sup> In these applications, it is highly desirable to achieve tunable luminescence in terms of luminescent intensity and wavelength (e.g, color in visible spectrum (VIS) region). Numerous studies had focused on tuning the properties of luminescence by changing phosphor's chemical compositions, crystal structure, phase, crystal size, and surface groups.<sup>[9-12]</sup> However, all those approaches are essentially an

1 *ex-situ* and irreversible process. Compared to modifying luminescent intensity, it is  
2  
3  
4 rare to modify and control the emitting wavelength of luminescence or color gamut in  
5  
6  
7 VIS of a phosphor with fixed composition by *in-situ* and dynamic approaches. The  
8  
9  
10 development of such a multi-color emitting material may lead to a broad spectrum of  
11  
12  
13 novel applications. [1-3, 6, 13-20] Recently, Liu's group realized a temporal full-color  
14  
15  
16 tuning through non-steady state upconversion photoluminescence via pulse width  
17  
18  
19 modulation of laser interaction with the samples.<sup>[21]</sup> They demonstrate dynamical  
20  
21  
22 fine-tuning emission of core-shell multiphase nanocrystal by controlling the optical  
23  
24  
25 excitation dynamics. Up to now, there has been very limited work in which both  
26  
27  
28 luminescence intensity and color gamut can be remotely modified, particularly in a  
29  
30  
31 single-phase phosphor. In our previous study, we presented a magnetic-induced  
32  
33  
34 luminescence (MIL) that light emission can be generated by low magnetic field  
35  
36  
37 excitation via strain-mediated coupling with piezophotonic phosphor  
38  
39  
40 (piezophosphor).<sup>[22, 23]</sup> The MIL intensity can be modulated by the magnitude and  
41  
42  
43 excitation frequency of magnetic stimuli in a reversible and dynamical manner.  
44  
45  
46

47  
48 **Xu et al. demonstrated pioneering works that strong visible light can be emitted from**  
49  
50  
51 **the mechanoluminescent samples upon stressing.**<sup>[20]</sup> It is noticeable that the significant  
52  
53  
54 development of piezophosphors, such as metal ion-doped ZnS have led to the  
55  
56  
57 implementation of a platform for achieving multicolor emissions.<sup>[7, 19, 24-28]</sup> The  
58  
59  
60

1 piezophosphor has a crystal structure which can create a piezoelectric potential  
2  
3  
4 (piezopotential) within the crystal lattice under an external stress.<sup>[29]</sup> The co-doped  
5  
6  
7 multiple metal ions in the piezophosphor feature ladder-like arranged energy levels,  
8  
9  
10 producing a set of emission wavelengths. In this work, we present a strategy based on  
11  
12  
13 the modulation of magnetic excitation frequency, offering exquisite control over the  
14  
15  
16 emission color of metal ion-doped ZnS piezophosphor. The experimental results  
17  
18  
19 reported here have provided an evidence of the temporal tuning of emitting  
20  
21  
22 wavelength covering three primary colors of red, green, blue (RGB) and white light  
23  
24  
25 under the remote modulation of low magnetic field strength. Therefore, our results  
26  
27  
28 will not only provide a new insight into tuning luminescence but also expand the  
29  
30  
31 applications of light-emitting materials and magnetic sensor.  
32  
33  
34

35  
36 In our design, polydimethylsiloxane (PDMS) is chosen as a matrix for packaging a  
37  
38  
39 flexible laminated composite, and also functions as delivering the generated strain.  
40

41  
42 The composite was fabricated with integration of one layer embedding soft  
43  
44  
45 ferromagnetic particles into PDMS, generating magnetostrictive strain under magnetic  
46  
47  
48 field. This magnetostrictive strain then triggers the adjacent PDMS layer embedded  
49  
50  
51 with various metal ions (e.g., Al, Cu)-doped ZnS piezophosphor to produce light  
52  
53  
54 emission, schematically illustrated in **Figure 1a**. **The ratio of phosphor and PDMS**  
55  
56  
57 **was optimized at 7:3. Such an optimized value was obtained from numerous**  
58  
59  
60

1 experiment results, which is a compromise between elastic module and luminescence.  
2  
3  
4 During the measurement process, when the intensity of magnetic field varies in the  
5  
6  
7 range of 2.0~3.5 kOe, the strain and stress from the composite increase monotonically  
8  
9  
10 with the applied magnetic field.<sup>[22]</sup> Since the magnetic elastomer shows a very low  
11  
12  
13 conceive field (~9 Oe) under the applied magnetic field strength (2~3.5 kOe), the  
14  
15  
16 strain rate should increase with the modulating frequency. The luminescent spectra of  
17  
18  
19 the piezophosphor were measured under different modulation frequency ( $f$ ) of  
20  
21  
22 magnetic field excitation (**Figure 1b**). When the excitation frequencies are set at no  
23  
24  
25 higher than 50 Hz, the composite produces a dominant green emission band peaked at  
26  
27  
28 503 nm. Intriguingly, when increasing modulation frequency of magnetic field with  
29  
30  
31 fixed strength, the emission shows a trend of an intensity increase in the shoulder  
32  
33  
34 peak at a range from 460 to 472 nm of blue emission band, while green emission the  
35  
36  
37 intensity at 503 nm exhibits a gradual suppression simultaneously. Remarkably, as the  
38  
39  
40 modulation frequency further increases, the suppression of emission intensity at 503  
41  
42  
43 nm continues, while the blue emission intensity continuously increases until the main  
44  
45  
46 spectrum peaked at around 460 nm ~ 472 nm when  $f = 470$  Hz. Therefore, we can  
47  
48  
49 achieve a dynamic and *in-situ* control over the piezophotonic emission wavelength  
50  
51  
52 simply by adjusting the modulation frequency of magnetic field excitation. Obviously,  
53  
54  
55 such a temporal tuning of emission wavelength differs greatly from conventional  
56  
57  
58  
59  
60  
61  
62  
63  
64  
65

1 methods where *ex-situ* ways (e.g., changes in chemical compositions of hosts and/or  
2  
3  
4 metal ion dopants of phosphors) are routinely employed for tuning emission  
5  
6  
7 wavelength.<sup>[24]</sup> Apart from the change in emitting wavelength, the luminescent  
8  
9  
10 intensity is varied with the modulation frequency. **Figure 1c** shows the integrated  
11  
12  
13 intensities of overall emissions as a function of  $f$  when the strength of applied  
14  
15  
16 magnetic field was fixed. As seen in the result, the integrated emission intensity  
17  
18  
19 increases with increment of excitation frequency. As the excitation frequency  
20  
21  
22 increases up to around 300 Hz, the emission intensity reaches its maximum value. The  
23  
24  
25 intensity of the luminescence declines afterwards with further  $f$  increment. We further  
26  
27  
28 visualize the frequency dependent emission color and intensity observed from our  
29  
30  
31 MIL composite. **Figure 1d** illustrates the photographs presenting the emission color  
32  
33  
34 varied from green to blue and intensity variation when  $f$  was modulated from 50 to  
35  
36  
37 470 Hz, according with the measured data as shown in Fig. 1c, respectively. It is  
38  
39  
40 known that color coordinates ( $x$ ,  $y$ ) are a measure of color properties in chromaticity  
41  
42  
43 diagram. As shown in **Table 1**, it is evident that the emissions in terms of color  
44  
45  
46 coordinates, peak wavelength and luminance of the samples can be effectively tuned  
47  
48  
49 by modulating the frequency of magnetic field excitation.  
50  
51

52  
53  
54 In order to study the blue and green components of the emissions, we further  
55  
56  
57 characterized the ZnS: Al, Cu emissions at the two characteristic wavelengths (472  
58  
59  
60

1 nm and 503 nm) selected in this work as shown in **Figure 2**. First, the two  
2  
3  
4 characteristic MIL emissions were measured under a sinusoidal modulated magnetic  
5  
6  
7 field with a constant magnetic strength of root-mean-square ( $H_{\text{rms}}$ ). The single  
8  
9  
10 wavelength transient characteristic of the switchable MIL with different modulated  
11  
12  
13 frequencies is shown in **Figure 2a**. When the magnetic field is switched on (i.e.,  
14  
15  
16  $H_{\text{rms}}= 3$  kOe), the total emission consisted of the emissions at the two selected  
17  
18  
19 wavelengths, namely blue component (472 nm) and green component (503 nm), rises  
20  
21  
22 until its saturated value, and then begins to fall towards zero as the magnetic field is  
23  
24  
25 subsequently switched off (i.e.,  $H_{\text{rms}}= 0$  Oe). As indicated in Figure 1, the green  
26  
27  
28 emission is more intense at low modulation frequency while the emission is peaked in  
29  
30  
31 blue spectrum region is gradually enhanced under high modulation frequency. **Figure**  
32  
33  
34 **2b** shows the rise times of blue/green emission as a function of excitation modulation  
35  
36  
37 frequency, where the rise time is defined here as the time duration for the emission  
38  
39  
40 intensity reaches its saturated values in response to the magnetic field switching. The  
41  
42  
43 result suggests that the rise time for both blue and green components becomes longer  
44  
45  
46 with the accretion of excitation frequency. Apart from the changes in rise time with  
47  
48  
49 the modulation frequency, the relative intensity of blue and green emissions can be  
50  
51  
52 adjusted by the modulation frequency. Since MIL intensity can be solely adjusted by  
53  
54  
55 excitation frequency, therefore, we study the relative intensities of the two  
56  
57  
58  
59  
60  
61  
62  
63  
64  
65

1 characteristic wavelengths to further investigate the excitation frequency depended  
2  
3  
4 peak shift. **Figure 2c** shows the relative emission intensities and emission ratio at the  
5  
6  
7 two characteristic wavelengths as a function of excitation frequency. The measured  
8  
9  
10 result is consistent with Fig. 1(b) that blue emission is enhanced with an increase in  
11  
12  
13 the frequency of excitation. Accordingly, the ratio of blue/green emission intensity  
14  
15  
16 also increases with the increment of excitation frequency. With this interesting result,  
17  
18  
19 one may expect that the emission spectrum and color can be modulated simply by  
20  
21  
22 alternating the frequency of magnetic field in an *in-situ* and reversible way. In  
23  
24  
25 addition to the frequency dependence of emission, the emission intensity is also  
26  
27  
28 affected by  $H_{\text{rms}}$  under different modulation frequency. Here the  $H_{\text{rms}}$  was varied by  
29  
30  
31 adjusting the separation between the magnet and the measured sample. **Figure 2d**  
32  
33  
34 shows the luminescence intensity at the two wavelengths versus the square of  $H_{\text{rms}}$   
35  
36  
37 applied to the sample. Apparently, the emission intensity of both blue and green  
38  
39  
40 components is linearly enhanced when increasing  $H_{\text{rms}}^2$ , which is similar to our  
41  
42  
43 previous observation on the sample applied with the magnetic field of low frequency  
44  
45  
46 ( $f < 50$  Hz).<sup>[22]</sup> The results can be understood that an increase in  $H_{\text{rms}}$  may cause the  
47  
48  
49 enhancement in the magnitude of strain, leading to detrapping more charge carriers  
50  
51  
52 and hence intensifying electron-hole recombination and luminescence. It is noticeable  
53  
54  
55 that such a good linear relationship between the output and input signals as shown in  
56  
57  
58  
59  
60  
61  
62  
63  
64  
65

1 Fig. 2d is very helpful for sensing application. The obtained results have the potential  
2  
3  
4 for developing magnetic-luminescence sensors which are capable of detecting  
5  
6  
7 magnetic field with a wide range of modulation frequency. Additionally, there is no  
8  
9  
10 observable spectrum shift of MIL as magnetic field strength varies within our  
11  
12  
13 measurement range.  
14  
15

16 **Figure 3** presents the proposed excitation temporal tuning mechanism of MIL from  
17  
18 ZnS: Al, Cu piezophosphor. Generally, when specific metal ions (Al and Cu) are  
19  
20 doped into host lattice of the piezophosphor (ZnS), non-equivalent substitutions take  
21  
22  
23 place, resulting in various kinds of defects. These defects generate several kinds of  
24  
25  
26 luminescent centers which can give rise to different color emission. Typically, sulfide  
27  
28  
29 vacancies ( $V_S$ ) are attributed to the lattice mismatch in the host crystal, which can  
30  
31  
32 form shallow donor state below the conduction band (CB) by acquiring a free electron.  
33  
34  
35  
36 In the meantime,  $Al^{3+}$  related defects  $Al_{Zn}$  create deeper donor levels under the CB  
37  
38  
39 which act as trapping centers for electrons, while the  $Cu^+$  related defects  $Cu_{Zn}$  carrying  
40  
41  
42 one negative charge act as the acceptor levels which can trap holes above the valence  
43  
44  
45 band (VB). These charge traps in different energy levels are bounded together by  
46  
47  
48 Coulomb interaction to form various luminescent centers in the form of  
49  
50  
51 donor-acceptor (D-A) pairs with discrete spatial intra-pair separation ( $r$ ).<sup>[30]</sup> As shown  
52  
53  
54  
55 in the left panel of **Figure 3**,  $r_1 < r_2$  where  $r_1$  and  $r_2$  represent the spatial  
56  
57  
58  
59  
60  
61  
62  
63  
64  
65



1 intra-pair-separation  $r$  of  $V_s$ -Cu<sub>Zn</sub> and Al<sub>Zn</sub>-Cu<sub>Zn</sub> pairs, respectively.<sup>[15]</sup> The relationship  
 2  
 3  
 4 between the emission photon energy and the intra-pair separation can be expressed as  
 5  
 6  
 7 [31]

$$10 \quad E(r) = E_g - (E_A + E_D) + \frac{q^2}{4\pi\epsilon_r r} \quad (1)$$

11 where  $E_g$  is the energy band gap,  $E_A$  and  $E_D$  represent the trap depth of acceptor and  
 12  
 13 donor, respectively;  $q$  is the electron charge, and  $\epsilon_r$  is the permittivity of phosphors.  
 14  
 15

16  
 17 In our experiment, when modulating magnetic field ( $H$ ) is applied to the composites,  
 18  
 19  
 20 the induced magnetostrictive strain ( $\epsilon$ ) will generate an inner piezoelectric potential in  
 21  
 22  
 23 the ZnS crystals. According to our previous study, the magnetostrictive coefficient  $\lambda$   
 24  
 25  
 26 the ZnS crystals. According to our previous study, the magnetostrictive coefficient  $\lambda$   
 27  
 28  
 29 can be written as,<sup>[22]</sup>

$$30 \quad \lambda = \frac{\partial \mathcal{E}}{\partial H} \quad (2)$$

31  
 32 **This is a parameter of the strain change with magnetic field.** This piezoelectric  
 33  
 34  
 35  
 36 potential induces an increase of electrostatic energy of electron in a charge trap, which  
 37  
 38  
 39 can be expressed as,<sup>[32]</sup>

$$40 \quad \Delta E = \frac{1}{k} \left( \frac{\lambda q H d_0}{\epsilon_r} \right)^2 \quad (3)$$

41  
 42 where  $d_0$  is the local piezoelectric constant,  $k$  is the force constant of host lattice.  
 43  
 44

45  
 46 Since piezophotonic emission is essentially a dynamic process, the relationship  
 47  
 48  
 49 between the change rate of the electrostatic energy and the applied magnetic field  
 50  
 51  
 52 excitation can be written as  
 53  
 54  
 55  
 56  
 57  
 58  
 59  
 60  
 61  
 62  
 63  
 64  
 65

$$\frac{\partial E}{\partial t} = \frac{2H \dot{H}}{k} \left( \frac{\lambda q d_0}{\epsilon_r} \right)^2 \quad (4)$$

where  $\dot{H} = \partial H / \partial t$  is the change rate of magnetic field, which is related to the strain change rate of the sample. When this induced strain sustains for a time  $t$ , the instantaneous trap depth  $E'_D$  of the charge trap would decrease to,<sup>[32]</sup>

$$E'_D = E_D - \frac{2H \dot{H}}{k} \left( \frac{\lambda q d_0}{\epsilon_r} \right)^2 t \quad (5)$$

From Eq. (1) and (5), it is conceivable that the binding energy of trapped electron decreases with increasing modulation frequency of magnetic excitation.

Hence, the phenomenon of tunable piezophotonic emission observed in Figure 1 can be interpreted as follows. When applying an alternating magnetic field to the composites, magnetostrictive strain induced piezopotential causes the band structure of ZnS to tilt and detrapping of electrons in the donor states takes place.<sup>[1, 15]</sup> At low modulation frequency of magnetic field (middle panel of Figure 3), mainly the deep charge traps  $Al_{Zn}$  sites are excited, leading to a green emission. As the frequency increases further (right panel of Figure 3), from Eq. 5, the trap depths of these donor states started to decrease. The shallower charge traps  $V_s$  therefore could be triggered and ionized even the magnitude of magnetic field remains constant, leading to an increase in the emission intensity at 472 nm. In addition, a small  $r$  of the  $V_s$ - $Cu_{Zn}$  pair leads to a large overlapping of the pair's wavefunction, resulting a high  $e^-h^+$

1 recombination rate. Meanwhile, the  $\text{Al}_{\text{Zn}}\text{-Cu}_{\text{Zn}}$  pairs with a larger  $r$  value will be  
2  
3  
4 saturated readily due to small overlapping of wavefunction under high excitation  
5  
6  
7 modulation frequency.<sup>[30, 33]</sup> Therefore, the green emission intensity saturates and  
8  
9  
10 declines as the excitation frequency increases, while blue emission will subsequently  
11  
12  
13 dominates in the luminescence spectrum, as shown in Figure 2c.  
14  
15

16 The *in-situ* color tunability by excitation frequency provides a convenient approach to  
17  
18  
19 implement full-color display. In addition, achieving real-time modulation of color  
20  
21  
22 temperature of white emission via reversible physical approach has been an attractive  
23  
24  
25 target for both fundamental research and numerous applications.<sup>[15, 25]</sup> As a proof of  
26  
27  
28 concept, we moved forward to combine the MIL composite with other fluorescence  
29  
30  
31 phosphors to achieve a real-time tunable white light and multicolor display. Through  
32  
33  
34 temporal control of the magnetic excitation, we can generate RGB display and white  
35  
36  
37 color with tunable color temperature (**Figure 4a**).  
38  
39  
40

41  
42 To construct the tunable white MIL emission, Ce doped  $\text{Y}_3\text{Al}_5\text{O}_{12}$  (YAG: Ce) was  
43  
44  
45 chosen by considering it is an efficient yellow phosphor excited by blue color  
46  
47  
48 radiation. The corresponding yellow emission from YAG: Ce is able to complement  
49  
50  
51 the blue light which escapes through in order to produce a white light. By combining  
52  
53  
54 MIL composite with YAG: Ce fluorescence phosphor, we have achieved white  
55  
56  
57 emission with correlated color temperature (CCT) ranging from 3700 to 5700 K via  
58  
59  
60

1 varying modulation frequency as shown in **Figure 4b**. The mixing YAG: Ce  
2  
3  
4 fluorescence phosphors with tunable piezophosphor produces white color possessing  
5  
6  
7 a wide range of specific color temperature. The modifying contributions of blue and  
8  
9  
10 yellow emissions thereby allow a reliable and continuous tuning of the emission color  
11  
12  
13 perceived by the naked eye, ranging from saturated yellow and warm-white to deep  
14  
15  
16 blue through cold-white lights. **Figure 4c** shows the change trends in CIE coordinates  
17  
18  
19 of the white emissions from the two composites samples with different ratio of YAG:  
20  
21  
22 Ce phosphor. These coordinates are close to the Planckian locus, and migrated in  
23  
24  
25 accordance to the mixing ratio of the composites and the temporal tuning. For  
26  
27  
28 example, in the composite with mixing ratio of 1:1 (ZnS: Al, Cu based composite:  
29  
30  
31 YAG:Ce), we observed a shift of CIE coordinate with increasing blue component  
32  
33  
34 under high frequency of magnetic field in a direction which was dictated by this  
35  
36  
37 weight ratio. As a result, the emission from the sample at  $f = 300$  Hz occurs at the CIE  
38  
39  
40  $(x, y) = (0.3352; 0.3354)$ , which is approximately standard white point, with an  
41  
42  
43 efficiency  $\eta$  of about  $0.0018 \text{ lm Oe}^{-1}$  ( $\eta \sim$  light emission output/magnetic field input  
44  
45  
46 strength). Therefore, an appealing feature of these white emissions is that the emission  
47  
48  
49 color temperature of a fixed sample can be controlled in reversible and *in-situ* route  
50  
51  
52 simply by varying the temporal of magnetic excitation alone, providing ground for  
53  
54  
55  
56  
57  
58  
59  
60  
61  
62  
63  
64  
65

1 It is well known that RGB is essential to achieve a full-color display. To develop a  
2  
3  
4 tri-colored *in-situ* tunable MIL with simultaneous persistence luminescence, we  
5  
6  
7 studied on coupling the MIL sample with a highly efficient red-emitting  
8  
9  
10 phosphorescence phosphor of  $(\text{Ca}_{1-x}\text{Sr}_x)\text{S}:\text{Eu}$ . We explored the possibility via a  
11  
12  
13 patterned array of ZnS: Cu based MIL composite combined with this red phosphor. A  
14  
15  
16 sinusoidal magnetic field excitation was applied to trigger the composite. The  
17  
18  
19  $(\text{Ca}_{1-x}\text{Sr}_x)\text{S}:\text{Eu}$  phosphorescence was employed to convert the green piezophotonic  
20  
21  
22 emission and displays a red colored logo of Hong Kong Polytechnic University  
23  
24  
25 **(Figure 4d)**. In addition, by incorporating both  $(\text{Ca}_{1-x}\text{Sr}_x)\text{S}:\text{Eu}$  phosphor into two  
26  
27  
28 kinds of MIL composite (ZnS: Cu green, and ZnS: Al, Cu blue), we have been able to  
29  
30  
31 generate a RGB display capable of converting magnetic energy to luminescence with  
32  
33  
34 emission chromaticity modulated in reversible and dynamical manner via controlling  
35  
36  
37 the excitation frequency **(Figure 4e)**. The RGB composite emission can be seen by  
38  
39  
40 the naked eyes.  
41  
42  
43  
44

45 **Figure 4f** shows the transient characteristic of the red emission from MIL composite  
46  
47  
48 incorporated with  $(\text{Ca}_{1-x}\text{Sr}_x)\text{S}:\text{Eu}$  persistence phosphor. In this measurement,  
49  
50  
51 magnetic field with  $f = 250$  Hz was initially switched on and retained at  $H_{\text{rms}} = 2.0$   
52  
53  
54 kOe for 1 min and subsequently switched off. The 640 nm emission rises almost  
55  
56  
57 instantaneously when the MIL excitation emission occurs and then begins to decay  
58  
59  
60  
61  
62  
63  
64  
65

1 exponentially when the magnetic field excitation ceases, resulting in a prolonged  
2  
3  
4 reddish persistence luminescence as expected. It is interesting to notice that this  
5  
6  
7 colour conversion not only broaden the color expression of MIL, but also prolonged  
8  
9  
10 the illumination of our composite after the stoppage of the excitation.

11  
12  
13 In summary, conventional tuning of the emitting wavelength and color from the  
14  
15  
16 materials are traditionally achieved by *ex-situ* and irreversible chemical approaches,  
17  
18  
19 namely changing the composition of the samples. In contrast, our novel approach  
20  
21  
22 reported in this work is based on a dynamic control of the piezophosphor's energy  
23  
24  
25 band structure and the trap depth of charge carriers, subsequently inducing activation  
26  
27  
28 or saturation of charge traps via a remote excitation. Experimentally, we have  
29  
30  
31 provided an evidence of tuning emission peak wavelength and color of ZnS: Al, Cu  
32  
33  
34 phosphors by modulating frequency of magnetic field excitation. Moreover, RGB  
35  
36  
37 full-color and white light with tunable color temperature are achieved via photon  
38  
39  
40 energy coupling with YAG: Ce and  $(\text{Ca}_{1-x}\text{Sr}_x)\text{S}:\text{Eu}$  persistence phosphor. The study  
41  
42  
43 provides a new insight and understanding on the piezophotonic emission mechanism.  
44  
45  
46  
47 Our new finding of the luminescent materials with ability to be accessed and  
48  
49  
50 modulated remotely will offer opportunities for applications in the fields of magnetic  
51  
52  
53 optical sensing, piezophotonics, energy harvester, non-destructive environmental  
54  
55  
56 surveillance, novel light sources and displays.  
57  
58  
59  
60

## Method

**Preparation of color-tunable MIL composites.** Metal ions doped ZnS microparticles with the average size of 23  $\mu\text{m}$  (Global Tungsten & Powders) were uniformly mixed into a PDMS matrix. Figure S1 shows the corresponding X-ray diffraction (XRD) pattern. The ratio of phosphor material: PDMS was maintained at 7:3. The cured piezophosphor doped PDMS (5 mm in length, and 1 mm in diameter) was embedded into magnetic elastomer (2 mm in length and 1 mm in diameter) consisted of soft ferromagnetic microparticle (Fe-Co-Ni alloy particle average sizes 100  $\mu\text{m}$ ) uncured PDMS in weight ratio 2.5:1. The samples were cured at 120  $^{\circ}\text{C}$  for 45 min. The resultant composite

### **Fabrication of the phosphor possessing RGB and tunable white MIL composite.**

The red colored Hong Kong Polytechnic University logo was patterned by screen printing (thickness 200  $\mu\text{m}$ ) the (SrS, CaS): Eu phosphor paste onto the top of a ZnS:Cu based MIL composite. Photoluminescence excitation (PLE) and photoluminescence (PL) spectra of (SrS, CaS): Eu are shown in Figure S2. This green MIL composite consisted of 16 composite rods, each with a diameter of 1 mm and a depth of 5 mm. For the element of individual multicolor volumetric MIL composite, the red phosphor paste was coated onto ZnS: Cu based MIL composite element rod.

1 The tunable white MIL composite was fabricated via homogenous mixing YAG: Ce  
2  
3  
4 phosphor with ZnS: Al, Cu piezophosphor. Figure S3 shows the PLE and PL spectra  
5  
6  
7 of YAG:Ce. Then this mixture was mixed into PDMS to form the tunable white MIL  
8  
9  
10 composite.

11  
12 **Optical characterization.** The MIL spectra and CIE coordinates of the MIL  
13  
14 composites were measured using a CCD camera (Ocean Optics USB4000) and  
15  
16 spectroradiometer (PR-655, Photo Research Inc.) with a detection spot of diameter  
17  
18  
19 5.25 mm. The MIL images were captured by a digital camera (Olympus Pen Lite E-  
20  
21  
22  
23  
24  
25  
26  
27 PL3).

28  
29 **Measuring of tunable MIL emission.** A homemade apparatus was used to generate  
30  
31 sinusoidal magnetic field at room temperature. A pulse width modulator (PWM) was  
32  
33  
34 used to modulate the frequency of the magnetic field. In detail, an electric motor  
35  
36  
37  
38  
39  
40  
41  
42  
43  
44  
45  
46  
47  
48  
49  
50  
51  
52  
53  
54  
55  
56  
57  
58  
59  
60  
61  
62  
63  
64  
65  
rotates a magnet with the rotation speed controlled by a pulse width modulation  
module. The magnet has a strong magnetic field along its radical axis, and it is rotated  
around the longitudinal axis of the magnet. The applied magnetic field strength on the  
composite is controlled via changing the distance between the MIL composite and the  
magnet. The green to blue color displayed was tuned by controlling the modulation  
frequency of the magnetic field. The magnetic field was set in the range of 2.5 ~ 3.5  
kOe, depending on the intensity of emission required.



1           **Acknowledgements**  
2  
3

4           The research was financially supported by the grants from Research Grants Council of  
5  
6  
7           Hong Kong (GRF No. PolyU 5005/13P) and National Natural Science Foundation of  
8  
9  
10          China (Grant No. 11474241).  
11  
12  
13  
14  
15  
16  
17  
18  
19  
20  
21  
22  
23  
24  
25  
26  
27  
28  
29  
30  
31  
32  
33  
34  
35  
36  
37  
38  
39  
40  
41  
42  
43  
44  
45  
46  
47  
48  
49  
50  
51  
52  
53  
54  
55  
56  
57  
58  
59  
60  
61  
62  
63  
64  
65

## References

- [1] X. Wang, H. Zhang, R. Yu, L. Dong, D. Peng, A. Zhang, Y. Zhang, H. Liu, C. Pan, Z. L. Wang, *Adv. Mater.* **2015**, 27, 2324.
- [2] Y. Zhang, G. Gao, H. L. Chan, J. Dai, Y. Wang, J. Hao, *Adv. Mater.* **2012**, 24, 1729.
- [3] J. Lee, P. W. Bisso, R. L. Srinivas, J. J. Kim, A. J. Swiston, P. S. Doyle, *Nat. Mater* **2014**, 13, 524.
- [4] S. M. Jeong, S. Song, S. K. Lee, N. Y. Ha, *Adv. Mater.* **2013**, 25, 6194.
- [5] H. Fang, X. Wang, Q. Li, D. Peng, Q. Yan, C. Pan, *Advanced Energy Materials* **2016**, 6, 1600829.
- [6] D. Tu, C.-N. Xu, A. Yoshida, M. Fujihala, J. Hirotsu, X.-G. Zheng, *Adv. Mater.* **2017**, 29, 1606914.
- [7] C. Pan, M. Chen, R. Yu, Q. Yang, Y. Hu, Y. Zhang, Z. L. Wang, *Adv. Mater.* **2016**, 28, 1535.
- [8] D. Peng, B. Chen, F. Wang, *ChemPlusChem* **2015**, 80, 1209.
- [9] G. Bai, M.-K. Tsang, J. Hao, *Adv. Opt. Mater.* **2015**, 3, 431.
- [10] C. Feldmann, T. Jüstel, C. R. Ronda, P. J. Schmidt, *Adv. Funct. Mater.* **2003**, 13, 511.
- [11] T. Dong, X. Chao-Nan, F. Yuki, Y. Akihito, *J. Phys. D: Appl. Phys.* **2015**, 48, 475105.
- [12] H. Li, N. Liu, X. Zhang, J. Su, L. Li, Y. Gao, Z. L. Wang, *Nano Energy* **2016**, 27, 587.
- [13] S. M. Jeong, S. Song, H. Kim, *Nano Energy* **2016**, 21, 154.
- [14] S. M. Jeong, S. Song, K.-I. Joo, J. Kim, S.-H. Hwang, J. Jeong, H. Kim, *Energy Environ Sci.* **2014**, 7, 3338.

- 1 [15] L. Chen, M.-C. Wong, G. Bai, W. Jie, J. Hao, Nano Energy **2015**, 14, 372  
2  
3 [16] Y. Sagara, T. Kato, Nat Chem **2009**, 1, 605.  
4  
5 [17] K. Y. Sasaki, J. B. Talbot, Adv. Mater. **1999**, 11, 91.  
6  
7 [18] W. Wu, Z. L. Wang, Adv. Mater. **2016**, 1, 16031.  
8  
9 [19] X. Han, W. Du, M. Chen, X. Wang, X. Zhang, X. Li, J. Li, Z. Peng, C. Pan, Z. L.  
10 Wang, Adv. Mater. **2017**, 29, 1701253.  
11  
12 [20] C. N. Xu, T. Watanabe, M. Akiyama, X. G. Zheng, Appl. Phys. Lett. **1999**, 74,  
13 1236.  
14  
15 [21] R. Deng, F. Qin, R. Chen, W. Huang, M. Hong, X. Liu, Nat. Nanotechnol. **2015**,  
16 10, 237.  
17  
18 [22] M. C. Wong, L. Chen, M. K. Tsang, Y. Zhang, J. H. Hao, Adv. Mater. **2015**, 27,  
19 4488.  
20  
21 [23] O. Graydon, Nat Photon. **2015**, 9, 558.  
22  
23 [24] G. Bai, M.-K. Tsang, J. Hao, Adv. Funct. Mater. **2016**, 26, 6330.  
24  
25 [25] D. Tu, C.-N. Xu, Y. Fujio, A. Yoshida, Light Sci Appl. **2015**, 4, e356.  
26  
27 [26] O. Chen, D. E. Shelby, Y. Yang, J. Zhuang, T. Wang, C. Niu, N. Omenetto, Y. C.  
28 Cao, Angew. Chem. Int. Ed. **2010**, 49, 10132.  
29  
30 [27] Y. Chen, Y. Zhang, D. Karnaushenko, L. Chen, J. Hao, F. Ding, O. G. Schmidt,  
31 Adv. Mater. **2017**, 29, 1605165.  
32  
33 [28] C.-N. Xu, T. Watanabe, M. Akiyama, X.-G. Zheng, Appl. Phys. Lett. **1999**, 74,  
34 2414.  
35  
36 [29] Z. L. Wang, NANO TODAY **2010**, 5, 540.  
37  
38 [30] D. Vij, *Luminescence of solids*, Springer Science & Business Media, **2012**.  
39  
40 [31] K. Era, S. Shionoya, Y. Washizawa, J. Phys. Chem. Solids **1968**, 29, 1827.  
41  
42 [32] B. P. Chandra, V. K. Chandra, P. Jha, Appl. Phys. Lett. **2014**, 104, 031102.  
43  
44  
45  
46  
47  
48  
49  
50  
51  
52  
53  
54  
55  
56  
57  
58  
59  
60  
61  
62  
63  
64  
65

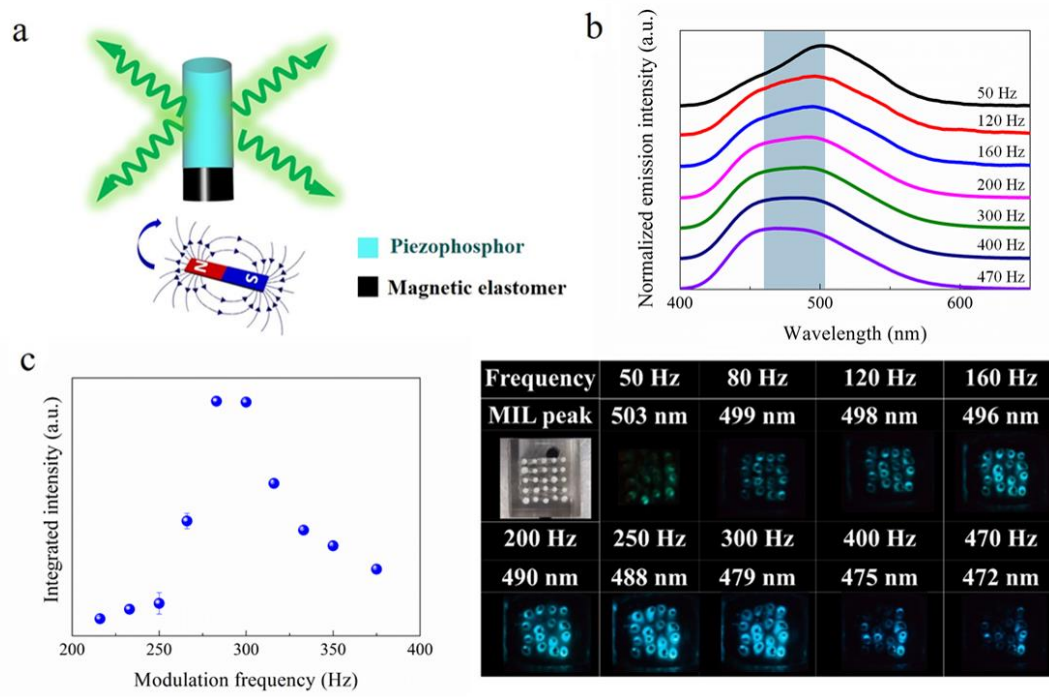


Figure 1 (a) Schematic illustration of metal ions (e.g., Al, Cu)-doped ZnS MIL composite when excited by a modulated magnetic field. (b) Normalized emission intensity of the composite under various frequencies, showing the emission wavelength tuning. (c) Integrated emission intensity as a function of the modulation frequency of magnetic field at fixed strength (2.0 kOe). (d) Photographs showing from green to blue color variation of the sample by changing the modulation frequency of magnetic field.

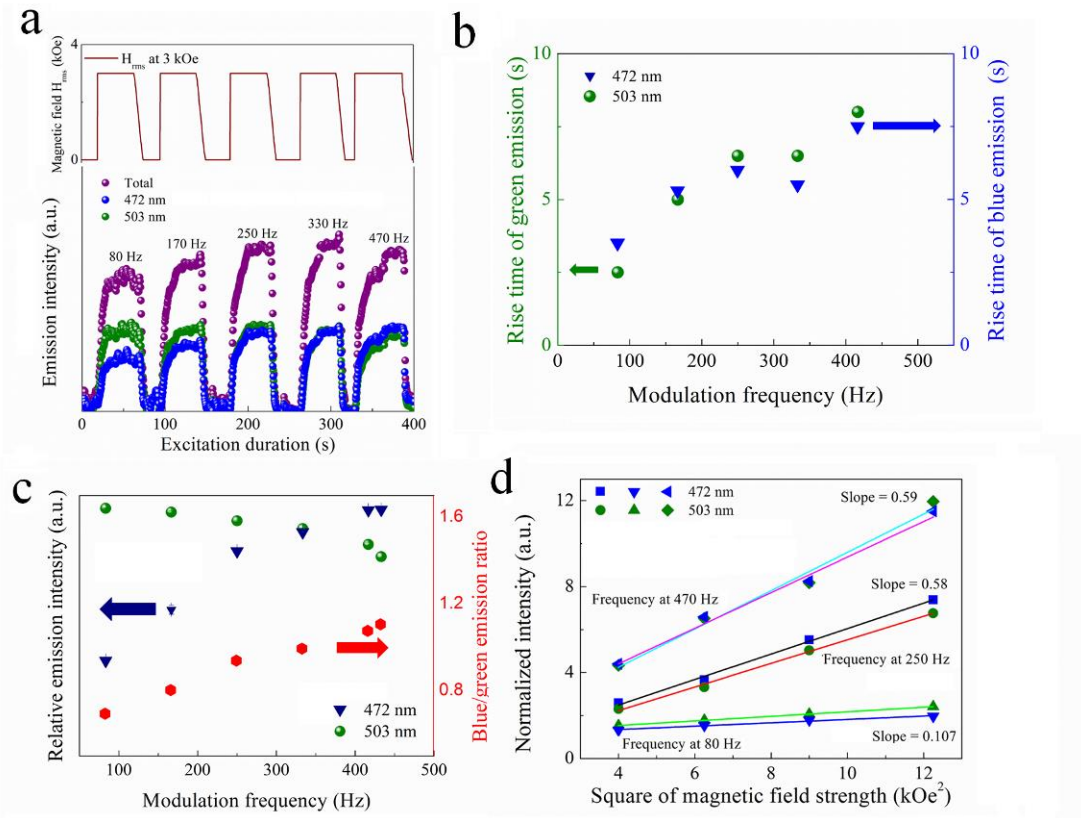


Figure 2 (a) Time dependent luminescence profiles of ZnS: Al, Cu emitting at 472 and 503 nm under sinusoidal magnetic field with various frequencies. (b) The rise time of 472 and 503 nm emission under different excitation modulating frequency. (c) The relative MIL intensity at 472 and 503 nm as a function of excitation frequency. (d) Emission intensity at 472 and 503 nm as a function of the square of magnetic field strength and the corresponding linear fittings.

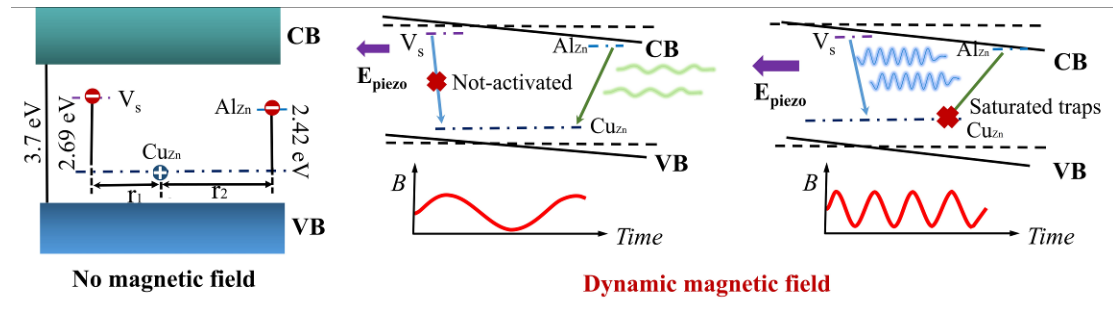


Figure 3 Schematic illustration of the mechanism responsible for temporal color tuning of MIL in ZnS: Al, Cu piezophosphor.

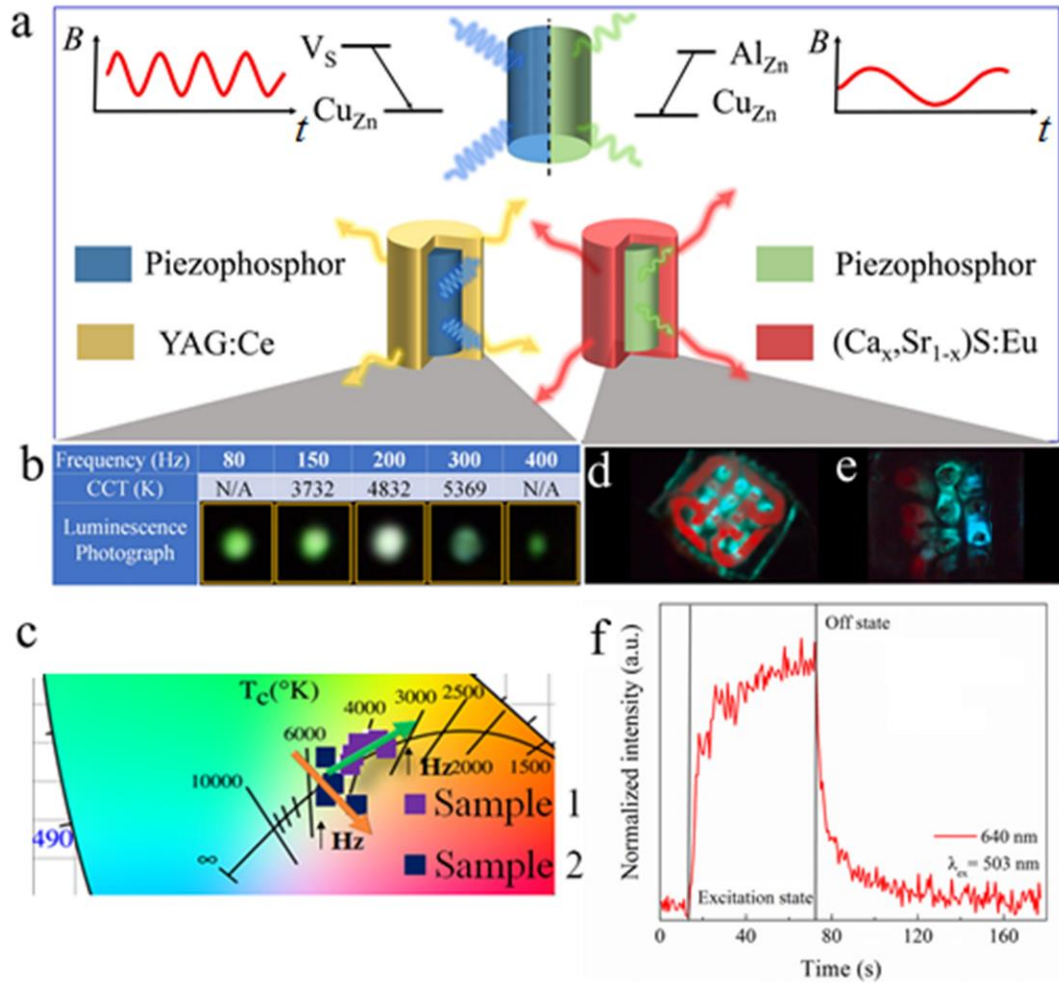


Figure 4 Demonstration of full-color display in MIL composite combined with other fluorescent materials. (a) Schematic of MIL full-color display realized by coupling MIL composite with different fluorescent materials. (b) Photographs of white emission with tunable color temperature under different modulation frequency of magnetic field from MIL composite mixed with YAG: Ce phosphor. (c) Enlarged CIE coordinates of adjustable white MIL emissions. (d) Multicolor MIL flexible composite combined with  $(Ca_x, Sr_{1-x})S:Eu$  displaying the logo of the Hong Kong Polytechnic University. (e) Display of RGB and white MIL emissions (f) The excitation and afterglow of red emission intensity at 640 nm as a function of time.

Table 1 CIE coordinates, emission peak wavelength and corresponding light intensity of ZnS:Al, Cu under different modulating frequency of magnetic excitation.

Frequency of excitation (Hz)	CIE (x,y)	Peak wavelength (nm)	Luminance (cd/m <sup>2</sup> )
80	(0.2129, 0.3470)	503	24
120	(0.1975, 0.2996)	496	30
160	(0.2216, 0.2679)	494	59
200	(0.2252, 0.2279)	489	82
300	(0.1841, 0.2239)	488	166
400	(0.1802, 0.2266)	479	64
470	(0.1627, 0.2108)	472	47



1 **The table of contents**

2  
3  
4 We present a strategy of temporal tuning of light-emitting wavelength and color in  
5  
6  
7 *in-situ* and reversible way, greatly differing from conventional approach. RGB and  
8  
9  
10 tunable white-light are demonstrated by modulating frequency of magnetic excitation.

11  
12  
13 The study provides a new understanding on luminescence mechanism. Our finding  
14  
15  
16 will offer opportunities in magnetic-optical sensing, piezophotonics, energy harvester,  
17  
18  
19 novel light sources and displays.  
20  
21

22  
23  
24  
25  
26 M.-C. Wong, L. Chen, Dr. G. X. Bai, Dr. L. B. Huang, Prof. J. H. Hao\*

27  
28  
29 Temporal and remote tuning of piezophotonic effect-induced luminescence and color  
30  
31  
32 gamut via modulating magnetic field  
33  
34  
35  
36  
37  
38  
39

